Vol. 03, Iss. 2 (2025) 258-265, DOI: 10.61552/JME.2025.02.010

JME

Journal of Materials and Engineering

www.jme.aspur.rs

Research article

Prediction of Tribological Characteristics of Biomaterials Using Artificial Neural Networks

M. Arulkumar[a,*], A. Krithik Raj[a], S. Saravanan[a], V. Muthukumar[b]

[a]*Department of Mechanical Engineering, Sri Venkateswara College Engineering, Sriperumbudur, India.*
[b]*Department of Mechanical Engineering, Saveetha Engineering College, Thandalam, India.*

Keywords:

Machine learning
Biomaterials
Response surface methodology
Sliding dry wear test
Coefficient of friction

* Corresponding author:

M. Arulkumar
E-mail: arulkumar@svce.ac.in

Received: 22 November 2024
Revised: 16 December 2024
Accepted: 29 January 2025

A B S T R A C T

Biomaterials are increasingly important in orthopaedic implants, particularly in Total Joint Replacement (TJR) procedures. Research has been conducted to identify suitable biomaterials for different joint replacements, with Total Hip Joint (THJ) and Total Knee Joint (TKJ) being the most common. Promising biomaterials for TJR include metals (such as Ti6Al4V, CoCrMo, and 316L SS), ceramics (like Al2O3), and polymers (such as UHMWPE). These materials are valued for their high strength-to-weight ratio, biocompatibility, corrosion resistance, and wear resistance. In this study, artificial intelligence was used to predict the tribological properties of these biomaterials. Experimental trials were conducted using a pin-on-disc tribometer to validate the artificial intelligence-based prediction of tribological properties, varying parameters such as applied load (40 N, 60 N and 80 N), sliding distance, and sliding velocity. With actual properties determined through machine runs. Experimental trials through a pin-on-disc tribometer were used to find the tribological properties of these biomaterials by varying applied load Sliding distance (1000 m, 1500 m, 2000 m) and sliding velocity (1.25 m/s, 2.1 m/s, and 3.2 m/s). Response Surface Methodology (RSM) was employed to predict the frictional behaviour of biomaterials by varying these input parameters. The predicted values were then compared with experimental results, showing that RSM could accurately predict the friction behaviour of the biomaterials with 95% accuracy. These findings demonstrate the potential of RSM as a predictive tool in biomaterials research, which can contribute to optimising tribological properties in medical implants and devices. This could lead to advancements in the design and application of orthopaedic implants.

1. INTRODUCTION

In the last thirty years, there has been significant progress in Total Joint Replacement (TJR) with metals, polymers, and ceramics. TJR focuses on advancing Total Knee Joint (TKJ) and Total Hip Joint (THJ) replacements to address issues such as metal reactions with body tissues, component loosening, and wear debris. The development of biomaterial technology aims to prevent failures

in TKJ and THJ, which can lead to wear and osteolysis [1-4]. This article provides an overview of the biomaterials used to minimize friction and wear. Metals, polymers and ceramics are widely used in biomedical applications such as internal support and biological tissue replacements, joint replacements, dental roots, orthopaedic fixation, and stents. The alloys primarily used in biomedical applications are 316L stainless steels, cobalt-chromium alloys, titanium alloys, ultra-high molecular weight polyethene and alumina as shown in Table 1 [5]. The lifetime of these biomaterials is determined by their abrasion and wear resistance. This causes severe infections in the body tissue due to its ion release and wear debris.[6, 7]

Table 1. Biomaterials in TJR [7].

Joint type	Material combination
Hip joint	CoCr Mo & UHMWPE
Hip joint	Stain steel & UHMWPE
Hip joint	Alumina &UHMWPE
Hip joint	CoCr Mo & CoCr Mo
Hip joint	Alumina & Alumina
Knee joint	CoCr Mo & UHMWPE
Knee joint	Stain steel & UHMWPE
Knee joint	Alumina & UHMWPE

Therefore, developing biomaterials with high wear resistance is critical to ensuring a long life for the biomaterial. This work shows that the surface modification techniques don't show a huge improvement in biocompatibility. Hence bioactive surface modification can sustain the need for bioimplants from accelerated tissue regeneration, antibacterial properties and controlled release and removal of debris from the biological system to the metal implants [8]. This report reviews the issues of THJ wear mechanisms and its methods of changing the surface topography of a ball-and-socket friction pair a metallic ball and a polymeric socket to identify the abrasion, fatigue and adhesion [9]. The recent technological developments in the field of tribological properties such as coefficient of friction and wear rate for the surface-modified metallic biomaterials including poly(ethylene glycol)-like (tetra glyme), diamond-like carbon, Ti–C: H, tantalum, CNT-reinforced hydroxyapatite, ultrahigh molecular weight polyethene, and titanium nitride coatings [10, 11]. The paper predominantly focuses on titanium-based alloys due to their enhanced mechanical properties, biological compatibility, and good tribological characteristics. Additionally, surface modification provides improved biocompatibility and corrosion resistance. [12-14]. This study conducted experimental work using a pin-on-disc tribometer to compare the performance of bioimplants under dry and wet lubricating conditions using sunflower oil. The comparison showed that the bioimplants exhibited a lower wear rate in the wet condition experiment compared to the dry condition experiment. This proves that lubrication is effective in reducing the coefficient of friction and wear rate. [15, 16]. In addition to advancements in biomaterial technology aimed at enhancing friction and wear properties with different biomaterial alloys, surface modification (coating and texturing), and lubrication, there have been notable strides in predicting tribological properties using artificial intelligence. [17, 18]. This paper introduces a feedforward backpropagation artificial neural network (ANN) model designed to accurately predict the specific wear rate and friction coefficient of aluminium-fly ash composites with 95% accuracy. [19]. The MRSM technique identified the optimal tribological behaviour for load and speed values in Ti alloy. The results indicate that the wear rate of Ti alloy is not directly proportional to the increasing load and speed values [20]. High bonding coatings of TiAlN were applied over surface texturing to achieve optimal tribological wear properties. A response surface methodology (RSM) study was conducted to observe the relationship between experimental results [21]. The bionic texture parameters obtained through response surface methodology (RSM) combined with lubrication enhance the bio-tribological properties of AISI 4140 steel. The optimized bionic texture parameters obtained through response surface methodology (RSM) significantly improve the bio-tribological properties [22-24].

2. FIELD TRIALS

2.1 Specimen Preparation

Biomaterials are obtained in the form of rods with the following chemical compositions: 1. Titanium Alloy (Ti6Al4V) – Titanium (Ti) 90%, Aluminium (Al) 6%, Vanadium (V) 4%, and other elements 0.1%. 2. Cobalt Chromium Alloy (CoCrMo) – Cobalt (Co) 60%, Chromium (Cr) 25%, Molybdenum (Mo) 11%, and other elements 4%. 3. Low Carbon Stainless Steel (316 L SS) – Iron (Fe) 65%, Chromium (Cr) 18%,

Nickel (Ni) 12%, Molybdenum (Mo) 2%, Carbon (C) 0.08%, and other elements 3%. 4. Alumina (Al2O3) – Aluminium (Al) 53%, Oxygen (O) 47%. 5. Ultra-High Molecular Weight Polyethylene (UHMWPE) – Carbon (C) 85% and Hydrogen (H) 15%.The procured biomaterials are machined using wire-cut Electric Discharge Machining (EDM) to the following dimensions: i) 28 mm x 10 mm and ii) 28 mm x 12 mm. These dimensions are chosen according to ASTM standard G90 [25] for conducting the sliding wear test using a pin-on-disc tribometer. The prepared specimens are depicted in Figure 01.

Fig. 1. Biomaterials.

2.2 Dry Sliding Wear Test

The dry sliding wear test was carried out using the Ducom TR pin-on-disc tribometer machine, as illustrated in Figure 2. a. The prepared specimens were tested on the pin-on-disc tribometer to assess biomaterials' friction and wear characteristics. The experimental trials were conducted at room temperature. Before placing the specimens into the pin holder of the tribometer, each specimen surface was cleaned using an Acetone solution to ensure a clean and scratch-free surface. A data acquisition system depicted in Figure 2. b was used to collect data from the tribometer. Sensors such as linear variable differential transformers (LVDT), accelerometers, friction sensors, load cells, thermocouples, and tachometers were employed to measure the variables to determine the tribological properties.

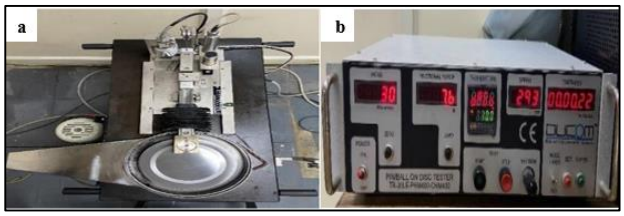

Fig. 2. (a) Pin-on-disc tribometer, (b) Data Acquisition System.

2.3 Response Surface Methodology

Researchers are trying to predict the tribological properties by identifying the most influential input parameters based on the output response. They are looking at various input parameters such as material composition, load, sliding velocity, and sliding distance to determine the levels of influence on these factors. They are using Design Expert software and response surface methodology to predict the friction properties of biomaterials. The correlation between the input and output parameters was determined using 2nd-order quadratic equations, as shown in Table 2.

Table 2. Input parameters for RSM

Material Type	Load (N)	Sliding Velocity (m/s)	Sliding Distance (m)
Ti6Al4V	40	1.25	1000
CoCrMo	60	2.1	1500
316 L SS	80	3.2	2000
Al_2O_3	--	--	--
UHMWPE	--	--	--

This research takes into consideration input parameters such as Load (A), sliding velocity (B), sliding distance (C), and material type (D). Equation (1) represents the connection between input variables and output response.

$$y = f\ (A, B, C, D) \qquad (1)$$

The quadratic model of y is used to identify where the primary target is located based on how the output response approaches or nears its optimum value, in addition to researching the full factor space. Relevant data are gathered for the quadratic models by applying a face-centred central composite design in machining tests based on response surface methodology (RSM). Table 3 shows the factorial design and its run number for the input factors and their responses.

Table 3. RSM design and its run numbers.

Input factors					Response
Run	**A**	**C**	**B**	**D**	**(μ)**
1	80	2880	3.2	UHMWPE	0.0969
2	80	1890	3.2	AL2O3	0.4893
3	100	1890	2.1	Ti6Al4V	0.3268
4	80	1125	1.25	AL2O3	0.4869
5	80	1125	1.25	AL2O3	0.4869
6	120	1890	1.25	UHMWPE	0.1667
7	120	2880	1.25	AL2O3	0.5998
8	80	2880	3.2	Ti6Al4V	0.2969
9	120	2880	1.25	CrCo	0.46
10	100	1890	1.25	316L SS	0.4191
11	80	1890	2.1	316L SS	0.3801
12	100	2880	2.1	CrCo	0.41

13	80	1890	1.25	CrCo	0.36
14	80	1125	3.2	316L SS	0.3698
15	100	2880	3.2	316L SS	0.4221
16	100	1125	1.25	UHMWPE	0.1262
17	100	2880	1.25	Ti6Al4V	0.3482
18	120	1890	2.1	AL2O3	0.5619
19	100	1125	2.1	CrCo	0.39
20	80	2880	1.25	316L SS	0.3912
21	80	1125	1.25	Ti6Al4V	0.2869
22	120	2880	3.2	AL2O3	0.5768
23	80	1125	1.25	Ti6Al4V	0.2869
24	120	1125	3.2	AL2O3	0.5521
25	120	1125	3.2	UHMWPE	0.1521
26	80	1890	3.2	AL2O3	0.4893
27	80	2880	3.2	CrCo	0.36
28	120	1125	3.2	Ti6Al4V	0.3521
29	120	2880	1.25	316L SS	0.4898
30	120	1125	1.25	Ti6Al4V	0.3599
31	120	1125	3.2	UHMWPE	0.1521
32	120	1125	3.2	316L SS	0.4421
33	80	1125	2.1	UHMWPE	0.0886
34	120	2880	2.1	UHMWPE	0.1795
35	120	1890	3.2	CrCo	0.42
36	120	1125	3.2	CrCo	0.41

3. RESULT AND DISCUSSION

3.1 Sliding Wear Test

Experimental work was conducted using a pin-on-disc tribometer wear test, and the resulting data was tabulated in Table 2. The data received from the data acquisition system was calculated based on equations 2, and 3.

$$\text{Sliding disance (mm)} = \frac{\pi \text{ x track diameter (mm) x disc speed (rpm) x testing time}}{60} \quad (2)$$

$$\text{Coefficient of friction } (\mu) = \frac{\text{Friction force (N)}}{\text{Applied load (N)}} \quad (3)$$

The coefficient of friction was calculated using equations 2 and 3 and then plotted in Figure 3. A three-axis graph was used to observe the impact of input-independent variables such as sliding velocity, sliding distance, and applied load for the biomaterials. In Figure 3a, the friction properties of the Al2O3 alloy are shown. It was observed that the applied load had the most significant impact on the resulting coefficient of friction while sliding velocity had the least impact. For example, at 80 N, the resulting friction value was 0.55, at 60 N it was 0.52, and at 40 N it was 0.48. Increasing the sliding distance from 1000 m to 2000 m tended to show increased trends in the coefficient of friction for different load conditions. In Figure 3b, the experimental friction values for 316L SS are presented. It was observed that at 80 N, the resulting friction value was 0.44, at 60 N it was 0.41, and at 40 N it was 0.37. Increasing the sliding velocity showed a slight deviation in improving friction values while increasing the load and sliding distance showed a reverse trend, increasing friction values. Figure 3c shows the machine run values for CoCrMo, which exhibited an increasing trend from 0.35 to 0.44 friction values as the applied load increased. Figure 3d shows the friction values of Ti6Al4V alloy, which varies from 0.28 to 0.33 as per the applied load. In Figure 3e, the friction values of UHMWPE range from 0.08 to 0.17 as the load increases. In Figure 3f, the average coefficient of friction is 0.53 for Al2O3, 0.42 for 316L SS, 0.39 for CrCoMo, 0.33 for Ti6Al4V, and 0.13 for UHMWPE.

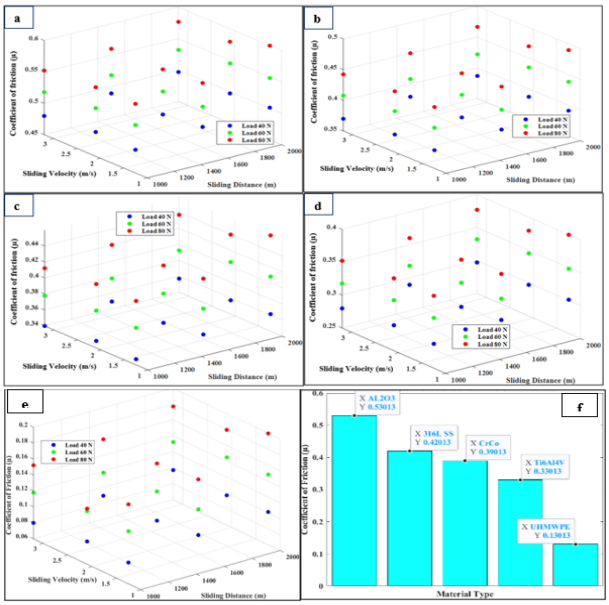

Fig. 3. Experimental results of (a) Al2O3, (b) 316L SS, (c) CrCoMo, (d) Ti6Al4V, (e) UHMWPE, (f) Coefficient friction.

3.2 ANOVA test

The performance of a model can be assessed using various fit summary parameters such as coefficient of determination (R-squared) and PRESS. In Table 4-8, you can find the highest polynomial order for model summary statistics, lack of fits, sum of squares, ANOVA model, and R-squared values. The fit statistical results indicated R-squared values of 1.0 and 0.9999 for cubic and quadratic models, respectively, to

coefficient friction responses. Furthermore, the lack of fit computation output diagnosed how well each sorted model fit the data, with a sequential sum of squares p-value of 0.0038. The ANOVA test was conducted to identify important terms in the model based on the low p-value criteria. A suitable cubic and quadratic mixture model was used to analyze the coefficient of friction. The analysis of variance revealed p-values of <0.0001 for the coefficient of friction, indicating significance. With a model F value of 3137.63, it is evident that the model is significant. The probability of obtaining an F value this large due to noise is only 0.01%. Model terms with "Prob > F" values less than 0.0579 are considered significant, including AB, AC, AD, BC, BD, and CD in this case. The Predicted R-squared of 0.9993 is in good agreement with the Adjusted R-squared of 0.9971, with a difference of less than 0.2. The ratio of adequate precision, which measures the signal-to-noise ratio, is 168.6952, indicating a strong signal. This model can effectively guide the design space.

Table 4. Model summary statistics for the coefficient of friction.

Source	Std. Dev.	R^2	Adjusted R^2	Predicted R^2	PRESS
Linear	0.0055	0.9987	0.9984	0.9979	0.0014
2FI	0.0038	0.9997	0.9993	0.9971	0.0019
Quadratic	0.003	0.9999	0.9995	0.9971	0.0019
Cubic	5.396E-03	1.0000	1.0000	0.9999	1.612E-03 Suggested

Table 5. Lack of fit for the coefficient of friction.

Source	Sequential p-value	Adjusted R^2	Predicted R^2
Linear	< 0.0001	0.9984	0.9979
2FI	0.022	0.9993	0.9971
Quadratic	0.0579	0.9995	0.9971
Cubic	0.0038	1.0000	0.9999 Suggested

Table 6. Sequential model sum of squares for the coefficient of friction.

Source	SS	df	MS	F-value	p-value
Mean vs Total	4.83	1	4.83		
Linear vs Mean	0.6674	7	0.0953	3137.63	<0.0001
2FI vs Linear	0.0007	15	0	3.15	0.022
Quadratic vs 2FI	0.0001	3	0	3.49	0.0579
Cubic vs Quadratic	0.0001	6	0	2.52	0.0034 Suggested
Residual	0	4	0		
Total	5.5	36	0.1527		

Table 7. ANOVA model for coefficient of friction.

Source	SS	df	MS	F-value	p-value
Model	0.668	22	0.0304	2152.59	< 0.0001
A-LOAD	0.0236	1	0.0236	1676.13	< 0.0001
B-SLIDING DISTANCE	0.0017	1	0.0017	117.84	< 0.0001
C-SLIDING VELOCITY	0.0004	1	0.0004	29.64	0.0001
D-MATERIALS	0.5778	4	0.1445	10240.75	< 0.0001
AB	0.0001	1	0.0001	9.45	0.0089
AC	0.0001	1	0.0001	6.51	0.0241
AD	0.0001	4	0	2.06	0.1451
BC	0.0001	1	0.0001	6.25	0.0266
BD	0.0001	4	0	0.959	0.4621
CD	0	4	0	0.8819	0.5014
Residual	0.0002	13	0		
Lack of Fit	0.0002	9	0		
Pure Error	0	4	0		
Cor Total	0.6682	35			

Table 8. R-squared calculations for the coefficient of friction.

Std. dev.	0.0038	R – squared	0.9997
Mean	0.3663	Adj. R-squared	0.9993
C.V %	1.03	Predicted R^2	0.9971
PRESS	0.0019	Adeq Precision	168.6952
−2 log-likelihood	-336.59	BIC	-254.16
		AICc	-198.59

The residuals of the model were found to closely follow a normal standard distribution near the regression line. This was indicated by the first diagnostic statistical plot. The externally studentized residuals are shown in this graph against the normal probability (%) of the outcome. It's important to look for clear patterns in the data for better analysis findings, such as curve-linear forms, which may suggest the need for transforming the target response. The figure displays the normal probability map for the coefficient of friction responses. In Figure 4a, the diagnostic assessment test shows that the residual assumption of constant variance is supported. The plot displays studentized residuals on the y-axis and anticipated outcomes on the x-axis.

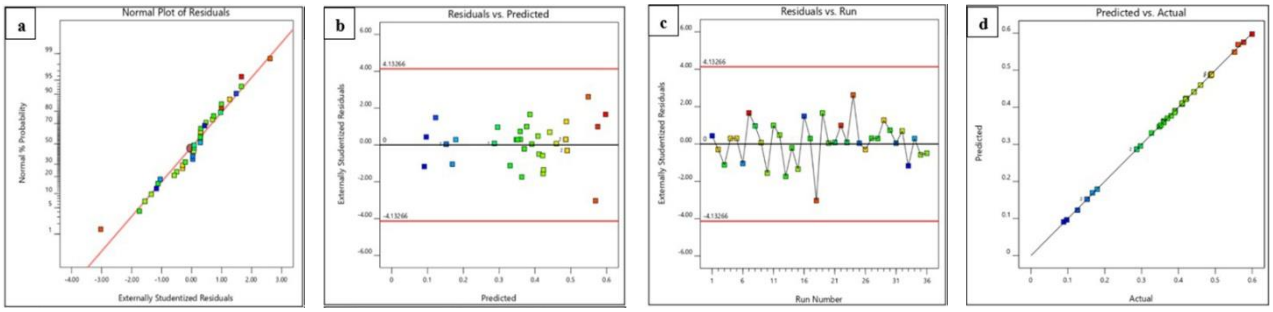

Fig. 4. ANOVA results, (a) Residual plot, (b) Residuals vs predicted, (c) Experimental vs predicted, (d) Predicted vs actual.

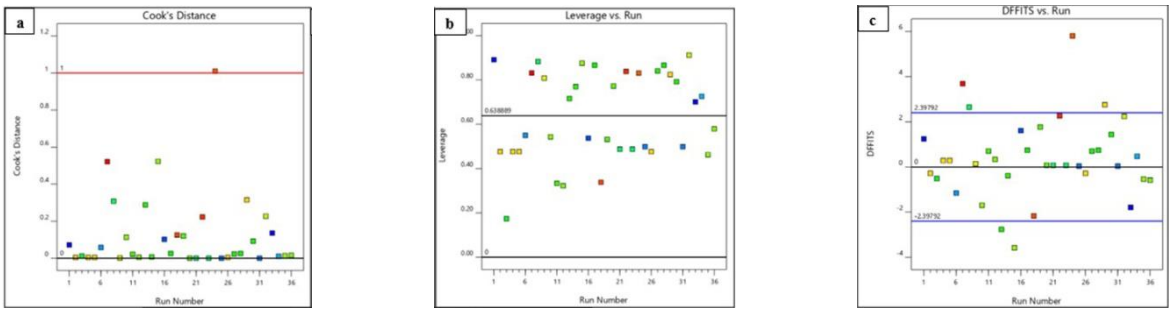

Fig. 5. ANOVA results, (a) cook distance, (b) leverage, (c) DFFITS.

The statistical findings reveal clustering around zero residual points. The coefficient of friction responses has maximum and minimum values of 4.132 and -4.132, respectively. The statistical diagnostic test examines how the order in which experiments are conducted impacts the target responses in comparison to the model's studentized residuals. Figure 4b illustrates this assessment plot, which identifies elements that may affect the criterion parameters during the experimental exercises. The design points were positioned close to the line of zero points and within the range of ± 4.132, indicating time-dependent parameters in a randomly scattered plot for coefficient friction response. This analytical figure depicts the behaviour of the real or experimental reactions on the x-axis about the RSM model predicted values on the graph's y-axis. Furthermore, as seen in Figure 4c, this statistical plot helps in assessing the link between the estimated and experimental outcomes, as well as the prediction accuracy performance of the RSM model to identify design points and groups that the model is undoubtedly unable to forecast. According to the results, the datasets for the square root responses of the coefficient of friction responses range from 0.1 to 0.6, respectively as shown in Figure 4d.

Regression statistics use Cook's distance to identify significant outliers in sets of independent or regressor variables. Figure 5a illustrates how Cook's distance is also used to identify areas or planes with high correlation, as well as experimental spots in the design that hurt the created RSM model. The graphical representation displays the 36 design numbers of experiments on the x-axis and the calculated Cook's distance value on the y-axis. The results showed that Cook's distance for the coefficient of friction ranged from 0 to 36. It's worth noting that the run number for experiment 26 was found to be above the 0–1 boundary line, while the other runs were situated below it. The leverage versus the experimental run statistical influence plot is shown in Figure 5b, with leverage points on the y-axis and experimental runs on the x-axis. The resulting leverage point ranges from 0 to 1, in which 0.638 signifies that the generated predictive model at the point of investigation fits the observation exactly. In Figure 5c, the DFFITS values are on the y-axis and the experimental values are on the x-axis, which measures the influence of each observation on the model's predicted values. The design point falls within the ± 2.39 range for the coefficient friction response, indicating its influence on the model's predictions.

4. CONCLUSION

During a sliding dry wear test, the impacts of sliding distance, sliding velocity, and applied load on the frictional properties of Ti6Al4V, UHMWPE, CoCrMo, 316L stainless steel, and Al2O3 were studied. A response surface methodology (RSM) study was conducted to obtain quadratic equations to predict the coefficient of friction and examine the materials' tribological behaviour. The following conclusions were drawn from the results of the sliding dry wear test and RSM:

1. The applied load has a greater influence on the tribological properties than sliding distance and sliding velocity. At an 80 N load, the coefficient of friction is higher for all materials.
2. Three different forms of biomaterials were used in the study: Metal-on-metal: Ti6Al4V exhibited friction values ranging from 0.33 to 0.28, CoCrMo exhibited friction values ranging from 0.35 to 0.39, and 316L SS exhibited friction values ranging from 0.37 to 0.42. Ceramic on metal: Al2O3 exhibited friction values ranging from 0.48 to 0.57. Polymer on metal: UHMWPE exhibited friction values ranging from 0.08 to 0.17.
3. RSM predictions indicated that sliding velocity and applied load have a more significant impact on the coefficient of friction than sliding distance.
4. The generated quadratic equations using RSM predicted the coefficient of friction for biomaterials with a 95% confidence level.

REFERENCES

[1] W. M. Mihalko, H. Haider, S. Kurtz, M. Marcolongo, i K. Urish, "New materials for hip and knee joint replacement: What's hip and what's in kneed?," *J. Orthop. Res.*, vol. 38, no. 7, pp. 1389–1399, Jul. 2020, doi: 10.1002/jor.24750.

[2] N. R. Patel i P. P. Gohil, "A Review on Biomaterials: Scope, Applications & Human Anatomy Significance," *Int. J. Emerg. Technol. Adv. Eng.*, 2012.

[3] M. A. Hussein, A. S. Mohammed, i N. Al-Aqeeli, "Wear characteristics of metallic biomaterials: A review," *Materials*, vol. 8, no. 5, pp. 2749–2768, May 2015, doi: 10.3390/ma8052749.

[4] "Comparison of the Various Groups of Metallic Biomaterials," 1AD.

[5] Z. R. Zhou i Z. M. Jin, "Biotribology: Recent progresses and future perspectives," *Biosurf. Biotribol.*, vol. 1, no. 1, pp. 3–24, Mar. 2015, doi: 10.1016/j.bsbt.2015.03.001.

[6] S. Ali *et al.*, "Biocompatibility and corrosion resistance of metallic biomaterials," *Corros. Rev.*, vol. 38, no. 5, pp. 381–402, Oct. 2020, doi: 10.1515/corrrev-2020-0001.

[7] M. Arulkumar, R. Prashanna Rangan, M. Prem Ananth, V. Srividhyasakthi, i R. Aaditya, "Experimental verification on the influence of surface texturing on biomaterials and study of its tribological characteristics," *Mater. Today Proc.*, Jan. 2023, doi: 10.1016/J.MATPR.2023.01.172.

[8] B. Priyadarshini, M. Rama, Chetan, i U. Vijayalakshmi, "Bioactive coating as a surface modification technique for biocompatible metallic implants: a review," *Adv. Mater. Process. Technol.*, vol. 5, no. 1, pp. 1–18, Oct. 2019, doi: 10.1080/21870764.2019.1669861.

[9] M. Niemczewska-Wójcik, "Wear mechanisms and surface topography of artificial hip joint components at the subsequent stages of tribological tests," *Measurement*, vol. 107, pp. 89–98, Sep. 2017, doi: 10.1016/j.measurement.2017.04.045.

[10] N. S. Manam *et al.*, "Study of corrosion in biocompatible metals for implants: A review," *J. Alloys Compd.*, vol. 695, pp. 1255–1270, 2017, doi: 10.1016/j.jallcom.2017.01.196.

[11] Z. A. Uwais, M. A. Hussein, M. A. Samad, i N. Al-Aqeeli, "Surface Modification of Metallic Biomaterials for Better Tribological Properties: A Review," *Arab. J. Sci. Eng.*, vol. 43, no. 11, pp. 5809–5834, Nov. 2017, doi: 10.1007/s13369-017-2624-x.

[12] M. Geetha, A. K. Singh, R. Asokamani, i A. K. Gogia, "Ti based biomaterials, the ultimate choice for orthopaedic implants - A review," *Prog. Mater. Sci.*, vol. 54, no. 3, pp. 397–425, May 2009, doi: 10.1016/j.pmatsci.2008.06.004.

[13] M. Long i H. J. Rack, "Titanium alloys in total joint replacement-a materials science perspective," *Biomaterials*, vol. 19, no. 18, pp. 1621–1639, 1998.

[14] M. Kaur i K. Singh, "Review on titanium and titanium based alloys as biomaterials for orthopaedic applications," *Mater. Sci. Eng. C*, vol. 102, pp. 844–862, Sep. 2019, doi: 10.1016/j.msec.2019.04.064.

[15] M. M. Mahat, N. Nadiah, M. Kamaldin, i A. A. Zulkornain, "Wear Characterization Analysis of Total Knee Replacement (TKR) Implant Materials," *Int. J. Eng. Technol.*, vol. 11, no. 4, pp. 345–356, 2022.

[16] Y. Liu, Q. Zhu, C. Wang, i J. Li, "Tribological behavior of CoCrMo artificial knee joint with symmetrically biomimetic textured surfaces on PEEK," *Opt. Laser Technol.*, vol. 157, p. 108774, 2023, doi: 10.1016/j.optlastec.2022.108774.

[17] Z. Mushtaq, M. Hanief, i S. A. Manroo, "Prediction of friction and wear during ball-on-flat sliding using multiple regression and ANN: Modeling and experimental validation," 2021.

[18] T. J. Griinke, "Development of an artificial neural network (ANN) for predicting tribological properties of kenaf fibre reinforced epoxy composites (KFRE)," 2013. [Online].

[19] K. R. Kumar, K. M. Mohanasundaram, G. Arumaikkannu, i R. Subramanian, "Artificial neural networks based prediction of wear and frictional behaviour of aluminium (A380)-fly ash composites," *Tribol. Mater. Surf. Interfaces*, vol. 6, no. 1, pp. 15–19, Mar. 2012, doi: 10.1179/1751584X11Y.0000000025.

[20] B. Kuriachen, K. P. Lijesh, i P. Kuppan, "Multi Response Optimization and Experimental Investigations into the Impact of Wire EDM on the Tribological Properties of Ti–6Al–4V," *Trans. Indian Inst. Met.*, vol. 71, no. 6, pp. 1331–1341, Jun. 2018, doi: 10.1007/s12666-017-1267-7.

[21] A. Muniyappan i P. A. Muthuvel, "Taguchi Optimisation of Friction and Wear Properties of Ti6Al4V Alloy Coated with TiAlN for Orthopaedic Applications," *Trans. FAMENA*, vol. 48, no. 4, pp. 17–32, 2024, doi: 10.21278/TOF.484059323.

[22] Q. Huang, X. Shi, Y. Xue, K. Zhang, i C. Wu, "Optimization of bionic textured parameter to improve the tribological performance of AISI 4140 self-lubricating composite through response surface methodology," *Tribol. Int.*, vol. 161, p. 107104, Sep. 2021, doi: 10.1016/J.TRIBOINT.2021.107104.

[23] G. Bergmann *et al.*, "Standardized loads acting in knee implants," *PLoS One*, vol. 9, no. 1, Jan. 2014, doi: 10.1371/journal.pone.0086035.

[24] D. Jandacka *et al.*, "Knee Joint Kinematics and Kinetics During Walking and Running After Surgical Achilles Tendon Repair," *Orthop. J. Sports Med.*, vol. 6, no. 6, Jun. 2018, doi: 10.1177/2325967118779862.

[25] A. Muniyappan *et al.*, "Enhanced Tribological Performance of Laser-Textured TiN-Coated Ti6Al4V Alloy Surfaces: A Comparative Study with Untextured Surfaces," *Processes*, vol. 13, no. 1, p. 204, Jan. 2025, doi: 10.3390/pr13010204.